



Decoding vibrational states of Concanavalin A amyloid fibrils



Federica Piccirilli ^{a,*}, Giorgio Schirò ^b, Valeria Vetri ^a, Stefano Lupi ^{c,d}, Andrea Perucchi ^{e,f}, Valeria Militello ^a

^a Dipartimento di Fisica e Chimica, Università di Palermo, Italy

^b CNRS–Institut de Biologie Structurale, Grenoble, France

^c INSTM Udr-Trieste ST, Trieste, Italy

^d Elettra-Sincrotrone Trieste S.C.p.A, Trieste, Italy

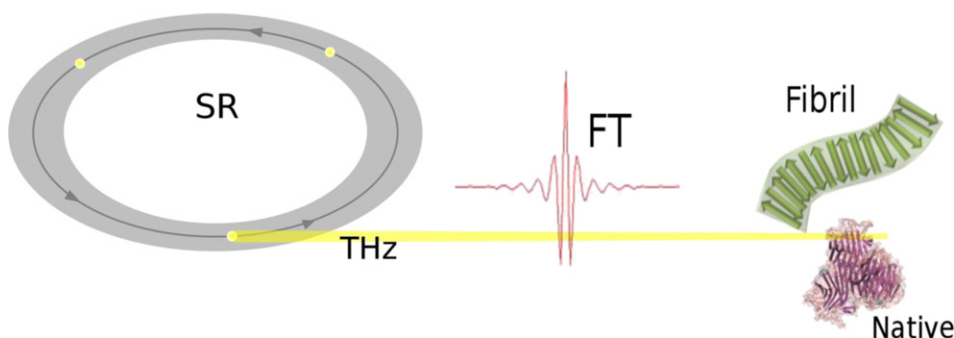
^e CNR-IOM, Italy

^f Department of Physics, Sapienza University of Rome, Italy

HIGHLIGHTS

- Simple coupling of low demanding techniques reveal amyloid structural details
- Raman peaks of fibrils at 1690 and 1620 cm^{-1} have been confirmed. These peaks have been rarely observed in Raman spectra.
- Fermi doublet show aromatic chains (Tyr) organization in fibrillar aggregates.
- We observe THz features of amyloid fibrils in comparison with native structure.
- THz spectroscopy highlights significant changes in hydration water around proteins building up fibril.

GRAPHICAL ABSTRACT



ARTICLE INFO

Article history:

Received 3 December 2014

Received in revised form 4 February 2015

Accepted 13 February 2015

Available online 21 February 2015

Keywords:

Amyloid

Fibrils

Raman

FTIR

Terahertz spectroscopy

ABSTRACT

Amyloid and amyloid-like fibrils are a general class of protein aggregates and represent a central topic in life sciences for their involvement in several neurodegenerative disorders and their unique mechanical and supramolecular morphological properties. Both their biological role and their physical properties, including their high mechanical stability and thermodynamic inertia, are related to the structural arrangement of proteins in the aggregates at molecular level. Significant variations may exist in the supramolecular organization of the commonly termed cross- β structure that constitutes the amyloid core. In this context, a fine knowledge of the structural details in fibrils may give significant information on the assembly process and on possible ways of tuning or inhibiting it. Here we propose a simple method based on the combined use of Fourier transform infrared spectroscopy and Fourier transform Raman spectroscopy to accurately reveal structural details in the fibrillar aggregates, side-chain exposure and intermolecular interactions. Interestingly, coupled analysis of mid-infrared spectra reveals antiparallel β -sheet orientation in ConA fibrils. We also report the comparison between THz absorption spectra of Concanavalin A in its native and fibrillar state at different hydration levels, allowing obtaining corroboration of peaks assignment in this range and information on the effect of amyloid supramolecular arrangement on the network dynamics of hydration water.

© 2015 Elsevier B.V. All rights reserved.

1. Introduction

The processes bringing proteins to associate and form amyloid aggregates, the structural properties of the aggregation products and

* Corresponding author.

E-mail address: federica.piccirilli@unipa.it (F. Piccirilli).

their biological relevance are central topics in the current biophysical and biochemical studies [1]. In suitable physicochemical conditions, proteins can modify their native conformation and associate to form supramolecular assemblies called amyloid fibrils, which are known to be involved in the etiology of many neurodegenerative disorders like Parkinson's and Alzheimer's diseases [2,3]. Amyloid fibrils consist of elongated structures whose spine is formed by multiple β -sheets that run parallel to the fibril axis [4] and represents the most stable state for the polypeptide chain [5]. These aggregates are characterized by peculiar physical and mechanical properties (like stability, high mechanical strength, ability to form gels and films) that make them particularly appealing for their application as nanomaterials [6]. The origin of these properties is certainly structure-dependent [6–9] and the possibility of modulating and manipulating them is linked to the knowledge of the fine structural details of amyloid fibrils. Detailed structural properties rule structural flexibility, surface topology and the distribution of hydrophobic regions in the surface of amyloids thus affecting their interaction with the environment, which is fundamental for their biological function [10,11]. Advances in biophysical technologies recently gave the possibility of revealing amyloid fibrils structure in detail and their supramolecular organization by means of high-resolution techniques as X-ray crystallography, solid-state nuclear magnetic resonance (SSNMR), and cryo-electron microscopy (cryoEM) [12–14].

Vibrational spectroscopy is known to be highly sensitive to protein structure. In particular, vibrational modes in the mid infrared region are sensitive to the secondary structural changes occurring upon amyloid fibrils formation [15–17], mainly in the amide I (amide I' in deuterated environment) band, centered at approximately 1660 (1650) cm^{-1} . At much lower frequency, vibrational modes falling in the far infrared region (THz range) can, in principle, provide information about long-range correlations, compactness and solvent-side chains coupling in proteins and, as a consequence, represent a powerful tool to investigate protein aggregates [8,18]. However, while much information is available about mid infrared absorption profiles of amyloids, only recently the study of THz collective vibrations modes in hydrated proteins has received attention. For example, low frequency modes, falling in the THz range, have been proposed to be involved in the optimization of biological energy transport by driving biochemical reactions and to be connected to the mechanical resistance of proteins and proteins aggregates [8,18,19]. THz spectroscopy provides also information about hydration water organization around proteins. Two primary types of protein/hydration water motions have been predicted to contribute to the low frequency spectrum of proteins: local librational motions (hindered rotations) of side chains and solvent, and large-scale correlated motions of the polypeptide backbone [19–24]. However, due to the collective character of THz modes, a molecular assignment of vibrational states often requires a complex normal mode analysis that takes into account the entire protein structure and, possibly, the interactions with the environment. A. Markelz and co-workers recently provided experimental evidence of narrow features of native egg white lysozyme in the 1–3 THz region and connected their spectral position and intensity to the structural state of the protein [18]. Concerning amyloid fibrils, it has been shown that a broad absorption peak associated to the fibrillar state of insulin exists in the region around 2 THz [25]. More recently, Schirò and co-workers showed, by means of inelastic neutron scattering, that fibrillation of glucagon induces a change in the shape of the THz spectrum, which is dependent on fibril morphology and hydration state [26].

Here we show how the exploration, by a combined use of Fourier transform infrared (FT-IR) and Fourier transform Raman (FT-Raman) spectroscopy, of the broad infrared spectrum from mid infrared (MIR) to the THz range may accurately reveal structural details of amyloid-like fibrils like secondary arrangement, hydration water properties, side-chain exposure and intermolecular interactions. Our results demonstrate how the coupled use of MIR and Raman spectra allows obtaining detailed structural insights on amyloid fibrils by means of

low demanding experimental and analysis techniques. The obtained information are used to support the interpretation of THz absorption spectra that reveal structure-dependent THz absorption modes of hydration water around amyloid fibrils which are not present in the native protein. This latter observation enables to speculate on the relationship between β -sheet rich aggregates and their environment.

The present study is focused on Concanavalin A (ConA) in both the native and the fibril state. ConA was chosen as a model system for its structural and aggregation properties. This protein has an “all- β ” secondary structure in the native state (N-ConA) and it may form long and thin fibrils (F-ConA) via a highly repeatable non-nucleated aggregation mechanism [27]. Interestingly, this protein shows a large structural homology to the human serum amyloid protein, generally present in all the in vivo fibril deposits [28] and it induces apoptosis on tumoral cells with a mechanism related to its aggregation [27,29].

2. Experimental methods

2.1. Sample preparation

Concanavalin A (type IV, L7647) was purchased from Sigma Aldrich and used without further purification. Con A amyloid fibrils in powder form have been prepared as described elsewhere [26,29]. Briefly 0.5 mg/ml of freshly prepared solution was incubated at 37 °C for 150 min in potassium phosphate buffer at pH 8.9 to obtain fibrils, then aggregation was quenched putting the sample in ice and samples were dialyzed against H_2O to remove buffer salts then they have been lyophilized. Dry powders have been dissolved in D_2O (10 mg/ml protein concentration) for FT-IR measurements. The aggregation state was verified by means of Thioflavin T test and confocal fluorescence microscopy.

Samples for THz spectroscopy were prepared as previously reported [30]. Briefly, to obtain dry samples ($h = 0$) samples were vacuum dried for 24 h and mass weight variation was measured to control hydration changes. The dried powders were then held in atmosphere of H_2O and left to reach the hydration level $h = 0.2$ and $h = 0.6$, determined by measuring the mass change. Dry and hydrated F-ConA and N-Con A were prepared in parallel with scrupulously identical treatments.

2.2. FT-MIR

Lyophilized powders were dissolved in D_2O (10 mg/ml) for FT-IR analysis. Infrared measurements were carried out on protein solutions with a Bruker Vertex 70 spectrometer equipped with a DTGS (doped triglycine sulfate) detector, in a sample compartment, under continuum purging in N_2 dry atmosphere. The protein solution was loaded into a liquid cell equipped with CaF_2 windows 2 mm thick; a mylar spacer 25 μm thick was used. Measurements were performed in transmission mode, in the 400–4000 cm^{-1} frequency range. Every measurement is the sum of 256 interferograms at 4 cm^{-1} resolution. Each spectrum is the average of five independent measurements. The contribution of the background was eliminated from Amide I' bands by subtracting buffer spectrum. The subtraction procedure was optimized in the region of H_2O bending, at about 1643 cm^{-1} . Amide I' bands were thus normalized.

2.3. FT-Raman

FT-Raman measurements were carried out with a Bruker Vertex 70 spectrometer equipped with a Ge N_2 -cooled detector, using an excitation laser with a wavelength of 1064 nm. Protein powders were loaded into a stainless steel (type 316L) sample holder. In order to avoid the damaging of the samples, the power of the excitation laser (at the source) was set around 30 mW. Measurements were performed in the 400–4000 cm^{-1} frequency range. Since we were interested in the spectral position of Raman features, we choose to work with non-deuterated

powders, in order to minimize anisotropic effects due to isotopic exchange producing band shifts. Data were analyzed in the 600–1880 cm^{-1} frequency range, where the main protein vibrational modes are found. Every measurement is the sum of 512 interferograms at 4 cm^{-1} resolution.

2.4. THz spectroscopy

FT-IR absorption measurements in the range between 10 and 130 cm^{-1} have been carried out using synchrotron light, collected with a He cooled detector (Bolometer). THz absorption spectra were recorded at the SSSI beamline at the Elettra synchrotron [20,33]. A standard infrared cell with variable path length has been used. The sample has been loaded into a sealed cell in the sample compartment of the Bruker spectrometer. To minimize etalon effects we used wedge diamond windows spaced of 15 μm for the measurements acquired at constant hydration. In order to minimize atmospheric absorption artifacts, measurements were performed in sample compartment, under vacuum.

2.5. Data analysis

Data were analyzed using Opus 6.5 (Bruker Optics). To evaluate the secondary structural changes induced by amyloid aggregation, we focused on amide I/I' band. Since amide I/I' frequencies are strongly affected by H-bonds and transition dipole coupling (TDC), they are highly sensitive to the secondary structure of proteins. A fitting procedure has been performed to identify the different contributions to the FT-IR spectra. The Fourier self deconvolution (FSD) technique (bandwidth 9 cm^{-1} and noise reduction 0.45) together with 2nd-derivative spectra, calculated using a Savitzky–Golay algorithm, with 17 smoothing points allowed identifying the different spectral components, which were used for initializing the fitting procedure [34,35]. The parameters used for initializing fitting curves were allowed to change without constraints during the minimization procedure. Voightian

profiles, that enable to describe absorption peaks as Gaussian convolutions of Lorentzian peaks, were used for modeling each absorption feature. The secondary structure assignments have been performed as described by Fabian and Mäntele [39]. 2nd-derivative Raman 2nd-derivative spectra, calculated using a Savitzky–Golay algorithm, with 21 smoothing points, have been used for qualitative deconvolution analysis. Tyrosines Raman peaks have been modeled through Gaussian profiles after baseline subtraction. Peak positions in THz spectra were determined by fitting them by Voightian profiles after suitable polynomial baseline subtraction. Since absolute absorption values are not discussed, all the experimental curves are reported in arbitrary units [31,32].

3. Results and discussion

3.1. Secondary structure of native and aggregated ConA

The analysis of F-Con A and N-Con A samples in deuterated solution was obtained through the analysis of amide I vibration.

Since four Amide I modes are produced by antiparallel β -sheet and just two by parallel β -sheet (see Fig. 1), the analysis of Amide I can give information on the reciprocal orientation of β -strands forming the sheet.

Fig. 2 reports the amide I' FT-IR band, between 1580 and 1710 cm^{-1} , of N-ConA (a) and F-ConA (b). The band of N-ConA is peaked around 1636 cm^{-1} , with a slight but significant shoulder around 1690 cm^{-1} .

The spectrum of native ConA is often used as a reference for FT-IR analysis of proteins for the high content of β -sheets of the protein; the peculiar shape of N-ConA Amide I is due to native β -sheets, but a closer inspection of the band also suggests the presence of intermolecular antiparallel β -sheets (see discussion in the following). As expected the spectrum of F-ConA in Fig. 2b reveals a prominent shoulder centered at about 1620 cm^{-1} typical of aggregated β -sheets with very strong intermolecular TDC and H-bonds [17,36]. It is worth noting that in the observed conditions ConA forms simple long and thin fibrils with no

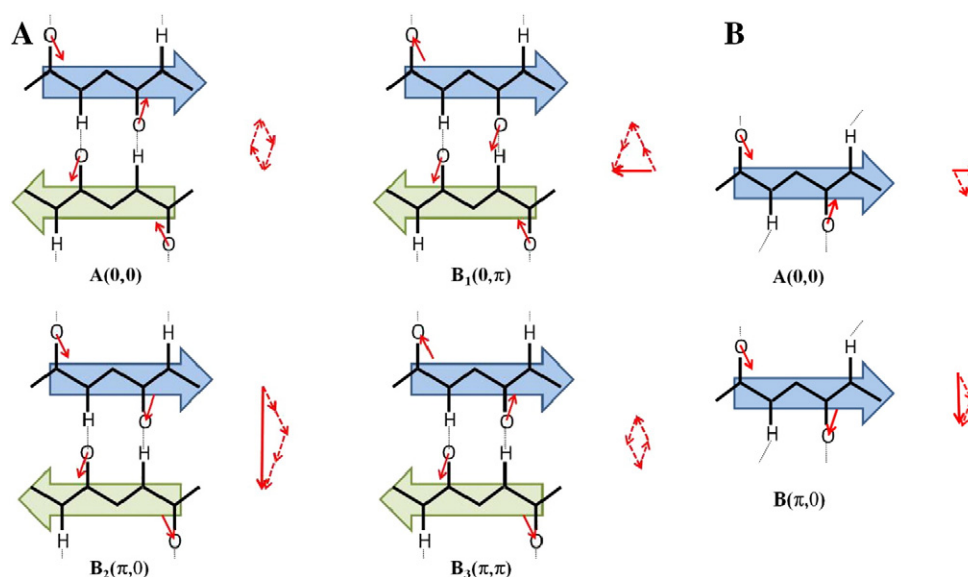


Fig. 1. Scheme of the amide I normal modes of antiparallel β -sheet (A) and parallel β -sheet (B) (modified from Barth et al. [36]). For antiparallel β -sheet the unit cell consists of 4 peptide groups while for parallel β -sheet it is composed of 2 peptide groups. The red arrows represent the contributions of the respective amide groups to the overall transition dipole moment (TDM). The dotted arrows on the right-hand side of every unit cell show the addition of the individual contributions to the overall TDM. According to theoretical calculations [37] and experimental evidences [38], two amide I (I') modes of antiparallel β -sheet, around 1630 cm^{-1} ($B_2(\pi,0)$) and 1690 cm^{-1} ($B_1(0,\pi)$) (1620 and 1685 cm^{-1} in deuterated environment) mainly contribute to the FT-IR spectrum, while an additional mode, absorbing around 1670 cm^{-1} ($B_3(\pi,\pi)$), should be the main peak present in the FT-Raman spectrum. Parallel beta-sheets are characterized by two spectral features: one in the infrared spectrum ($B(0,\pi)$), due to out of phase oscillators and absorbing around 1630 cm^{-1} (1620 in deuterated environment), and another one ($A(0,0)$), due to in phase coupled oscillators, typically observed in the Raman spectrum around 1660–1670 cm^{-1} .

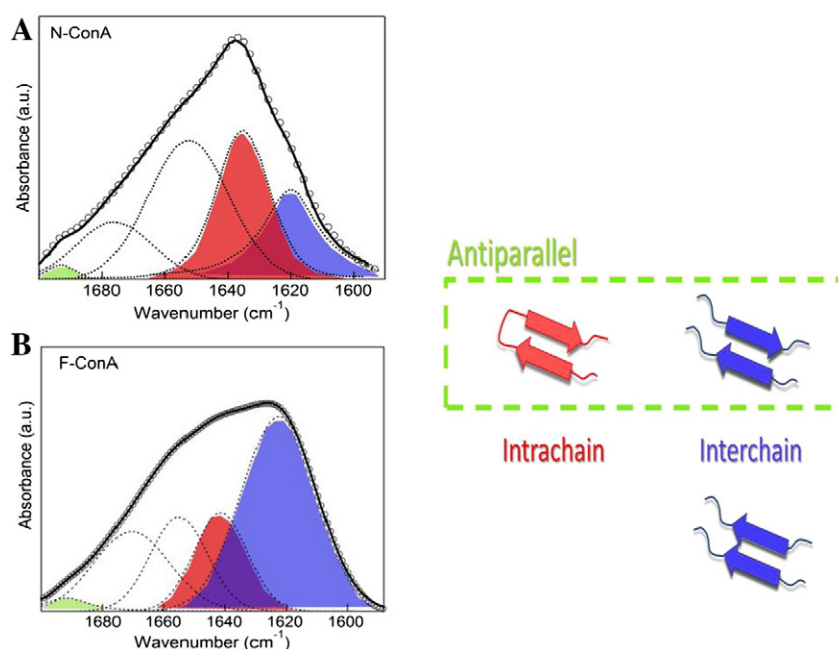


Fig. 2. FT-IR normalized Amide I' spectra of N-ConA (a) and F-ConA (b) in D₂O. The intramolecular β -sheet moieties are signaled by the presence of the peak absorbing at about 1639 cm^{-1} (enlightened in red), while the peak at about 1618 cm^{-1} (enlightened in blue) hints at the presence of aggregated β -sheet. The two mentioned absorptions can be ascribed to the $B_2(\pi,0)$ mode of β -sheet while the peak at about 1689 cm^{-1} , enlightened in green, can be ascribed to the $B_1(0,\pi)$ mode and is usually considered as hallmark of antiparallel β -sheet.

superstructures [27]. This allows singling out information on fibril molecular structures at the level of the amyloid backbone.

In order to detail information on aggregate molecular structure we present the deconvolution of the FT-IR spectra resulting from the analysis described in the *Experimental methods* section. As suggested by 2nd-derivative spectra, whose detailed analysis is presented below, we modeled the data using five absorption components. In line with what reported in the literature [39], the main components of these spectra can be assigned to specific structures, as reported in Table 1.

The main secondary structural moiety in N-ConA is found at 1634 cm^{-1} and represents 34% of the total spectrum area, respectively. This absorption peak corresponds to the vibrational motions of the backbone amide in the intramolecular β -sheet conformation. An intense component is also observed at 1618 cm^{-1} (21% of total area), associated to β -sheets with strong TDC and H-bonds [17,36,40].




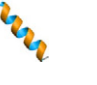



This can be rationalized considering that in native conditions, ConA dimer is stabilized through a 12-stranded β -sheet resulting from the antiparallel inter-monomers alignment of two flat 6-stranded β -sheets, one from each monomer [41].

Several theoretical models correlate the spectral position of Amide I band in β -sheet structures to detailed structural parameters as for instance to the number of strands composing the sheet as well as to the twist and the hydration state of the polypeptide chains of strands [42–44].

In particular, it is well assessed that due to the strong coupling between groups in adjacent chains, the higher the number of strands in the sheet the lower the amide I frequency [36,37,42]. Accordingly, we associated the low frequency absorption at about 1618 cm^{-1} (highlighted in blue) to the 12-stranded β -sheet stabilizing the ConA dimer. The comparison of the relative band area, 21%, of this component, and the measured fraction of the polypeptide chain involved in the formation of the 12 stranded β -sheet (about 28%), supports the performed assignment. The analysis reveals also secondary structural components at 1652 cm^{-1} , and 1676 cm^{-1} , hallmarks of random structures or loops and turns and loops. The quantitative assignment of secondary structures is reported in Table 2.

A minor component (2%) at about 1693 cm^{-1} (highlighted in green), due to the $B_1(0,\pi)$ mode resulting from excitonic splitting of β -sheet vibrations [36], signals the β -sheet antiparallel conformation typical of the ConA native structure. According to the crystal structure of native Concanavalin A found by Hardman and Ainsworth [41] (PDB 3CNA), around 40% of the polypeptide chain is involved in the formation of β -sheet, 10% in turns, 20% in bends and 30% is not involved in any secondary structure. The presented structural evaluation seems thus to over-estimate the β -sheet content of the protein of about 10% in respect to the structure obtained from diffracting crystals. This can be justified by considering that proteins in solutions have been here

Table 1
Secondary structure assignments [36–40] for amide I FT-IR frequencies of proteins.

							
	β -sheet ^a	β -sheet	Random	α -helix	Turn & loops	β -sheet	β -sheet ^a
H ₂ O	1620–1630	1626–1636	1650–1658 ^b	1650–1658	1670–1695	1680–1690	1690–1695
D ₂ O	1611–1620	1620–1634	1642–1650	1650–1658	1665–1690	1670–1680	1680–1689

^a In aggregates.

^b Depending on protein structure, absorption peaks of can be also found loops in this same spectral range.

Table 2
Secondary structure assignment for N-ConA and F-ConA derived FT-IR data analysis (see Fig. 2).

Secondary structure assignment	N-ConA		F-ConA	
	Position (cm ⁻¹)	Structure content %	Position (cm ⁻¹)	Structure content %
β-sheet (aggregated)	1618	21%	1620	39%
β-sheet (intramol)	1634	34%	1639	16%
Random coil	1652	22%	1652	21%
Turn	1676	21%	1665	19%
β-sheet ^a	1693	2%	1690	5%

^a Both of native and aggregated protein.

studied and that the experiments have been conducted at relatively high protein concentration.

The amide I' band of F-ConA is red-shifted with respect to N-ConA of about 12 cm⁻¹, and less symmetric than the native state spectrum. The main band component, at about 1620 cm⁻¹ (39% of the total area—highlighted in blue) corresponds to the vibrations of β-sheet moieties with strong coupling between peptides, typical of multistranded

β-sheet structures. The quantitative structural evaluation performed is reported in Table 2.

According to the assignments reported above, three hallmarks of intramolecular structures are observed at about 1639 cm⁻¹ (highlighted in red), 1652 cm⁻¹ and 1665 cm⁻¹, respectively assigned to intramolecular β-sheet (16%), random coils (21%), and turn and other intramolecular structures (19%) [24]. Notably, we observed an absorption component at about 1690 cm⁻¹ also in the F-ConA spectrum (5% of amide I' band). This finding, together with the presence of the 1620 cm⁻¹ peak, indicates the antiparallel conformation of a fraction of β-sheets composing the ConA fibril structure. The presence of the peak at about 1639 cm⁻¹ in F-ConA sample residual shows that native like intra-molecular β-sheet is retained upon aggregation, together with random coil and loops as indicated by a common peak at about 1652 cm⁻¹ found in both samples.

This is in line with the previous observation that ConA fibrillation essentially proceeds via a non-nucleated formation of intermolecular β-sheets, without any significant structural change not paralleling supramolecular aggregation process [45].

The detailed analysis of Amide I' reveals structural features of the samples that can be complemented by the information contained in

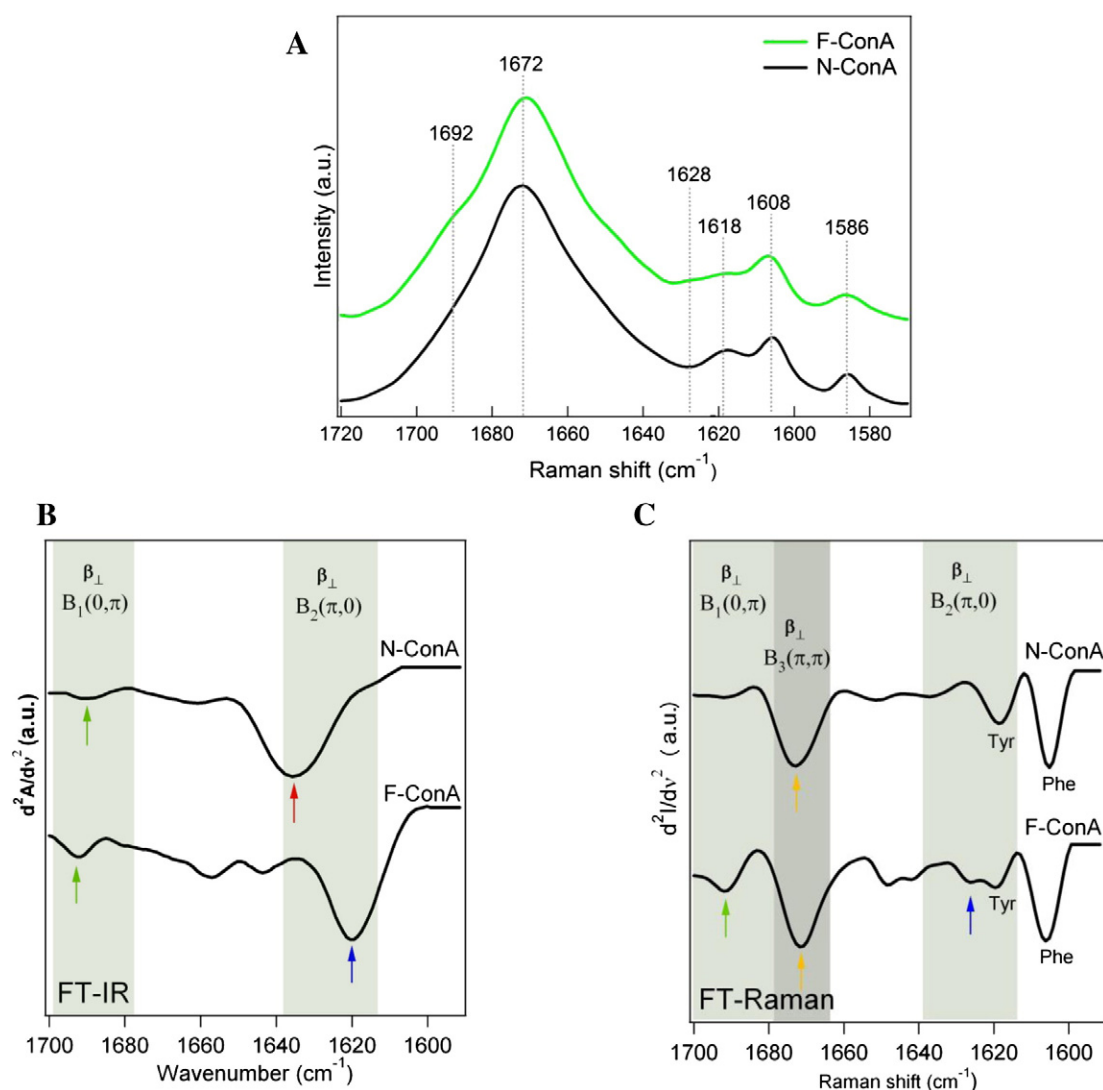


Fig. 3. Amide I FT-Raman of N-ConA and F-ConA in powder form (A). F-ConA band shows the presence of two shoulders at about 1628 and 1692 cm⁻¹ that are not present in N-ConA, thus suggesting the presence of additional antiparallel β-sheet in proteins structure. 2nd-derivative FT-IR spectra of N-ConA and F-ConA in the spectral region of Amide I' band (B) and FT-Raman 2nd-derivative spectra of N-ConA and F-ConA in the region of Amide I band (C). The red, green and blue arrows highlight the vibrational modes, described in Fig. 1 and already observed in absorbance spectra reported in Fig. 2, while the yellow arrows refer to the main absorption peak observed in Raman spectra (B₃(π,π)) reported in (a).

Fig. 3a, which reports the FT-Raman spectra of N-ConA and F-ConA samples in the 1550–1710 cm^{-1} region. As it is evident, the main peak, attributable to amide I band (1610–1710 cm^{-1}), is centered at about 1672 cm^{-1} for all samples and it is quite symmetric.

As it can be observed in Fig. 1, the Raman peak around 1670 cm^{-1} can be alternatively associated to B_3 (π, π) mode of antiparallel β -sheet moieties or to $A(0,0)$ mode of parallel β -sheets. FT-Raman spectra, which are usually not recognized to distinguish secondary structure details, reveal deep differences between F-ConA and N-ConA both at a first inspection and provide structural insights after suitable analysis. In particular, two additional shoulders can be observed in F-ConA at about 1692 cm^{-1} and 1628 cm^{-1} . The two shoulders in the F-ConA spectrum can be associated to the components revealed by FT-IR at about 1690 and 1620 cm^{-1} . The slight difference in the spectral position is due to isotopic exchange experienced by proteins in deuterated environment. Since the peak at about 1690 cm^{-1} is unequivocally linked to the $B_1(0, \pi)$ mode, it indicates the presence of an increased amount of antiparallel β -sheet in the sample.

The coupled observation of 2nd-derivative minima of the FT-Raman (Fig. 3b) and FT-IR (Fig. 3c) spectra of N-ConA and F-ConA, allows confirming the structural evaluation of the samples described above and clearly reveals that both Raman and FT-IR data show well defined features occurring at similar spectral positions. Indeed, the coupled observation of the 1692 cm^{-1} (green), 1669 cm^{-1} (yellow) and 1628 cm^{-1} (blue) features, which give details on the β -sheets structural organization, allows us to conclude that all the β -sheet modes, two of which are revealed by FT-IR, are clearly detectable in the FT-Raman spectrum of F-ConA.

3.2. Aromatic chain environment

Further information on the supramolecular organization of the aggregates structures arise from the analysis of the spectral features relative to aromatic side chains and present in the lower wave numbers region (1620–1580 cm^{-1}) of FT-Raman spectra reported in Fig. 3. In particular three features were observed at about 1618 cm^{-1} , 1609 cm^{-1} and 1585 cm^{-1} . The 1620–1580 cm^{-1} frequency range is typical of phenyl ring vibrational modes. The observed peaks can be attributed to the overlap of tyrosine (Tyr) and phenylalanine (Phe) residue contributions (1618 and 1585 cm^{-1} , respectively), with a possible contribution from tryptophan (Trp) residues (1609 cm^{-1}) [46,47]. Notably the feature at 1618 cm^{-1} , which can be assigned to intermolecular β -sheets (with all warnings described above) in FT-IR spectra of amyloid aggregates, is due to Tyr aromatic side chains in FT-Raman spectra.

In Fig. 3a it is possible to observe a broadening of Phe/Tyr peaks at 1608 and 1585 cm^{-1} relative to F-ConA with respect to N-ConA. This effect can be ascribed to differences in the aromatic side chain environment in the native and fibrillar state.

3.3. Tyrosine Fermi doublet

The FT-Raman spectra in the tyrosine Fermi resonance doublet region of ConA spectra are reported in Fig. 4, after suitable baseline subtraction, together with relative spectral deconvolution. In this region, ranging between 800 and 900 cm^{-1} , the Raman spectrum contains Tyr features that selectively probe the side-chain environment. In particular, the exposure of Tyr residues to water on the protein surface can be determined through the observation of a Fermi resonance, producing the doublet 830–860 cm^{-1} , between ring-breathing vibration and over-tone of an out-of-plane ring-bending vibration for the para-substituted benzene [46].

The study of these features for a number of proteins revealed that the ratio $R_{\text{Tyr}} = I_{860}/I_{830}$ (where I_{860} and I_{830} are the intensities of the Tyr doublet at 860 and 830 cm^{-1} , respectively) is strongly sensitive to the nature of hydrogen bonding or to the state of the dissociation of the phenolic hydroxyl group [46,47]. For this reason, this parameter

can be used to quantify the level of “buried” and “exposed” Tyr moieties. In particular, in exposed Tyr residues, where the phenolic hydroxyl group acts as a very weak hydrogen bond donor, R_{Tyr} is higher than 1; in Tyr residues buried into hydrophobic environments, R_{Tyr} is lower than 1. In order to quantify the exposure level of these aminoacids, and in turn to have more information on aggregates supramolecular organization, we calculated the R_{Tyr} values relative to the different samples. The R_{Tyr} parameter gives useful information on the exposure of the Tyr residues but it must be taken in consideration together with the shape of the relative spectra. Indeed, as evident in Fig. 4, the peak at about 860 cm^{-1} , attributable to exposed Tyr residues, is structured in the case of F-ConA sample, thus indicating different and more heterogeneous environments of aromatic residues.

In order to get quantitative information we applied a deconvolution procedure as described in the *Experimental methods* section. The peaks of the Tyr doublet of N-ConA and F-ConA are observed at about 853 and 828 cm^{-1} . However, it is evident that a third peak is present at about 860 cm^{-1} , with a larger intensity in aggregated samples. This feature, as already reported [47,48], clearly reveals the presence of a double population of exposed Tyr residues. On the basis of the results in Fig. 4, we obtained detailed information on the structure of ConA aggregates, in particular on Tyr residues, which were not obtained with other techniques. A fraction of Tyr residues, which are buried in the native state, becomes exposed to hydration water in the fibril state. This finding is in agreement with a recent neutron scattering study, where the increased exposure of side-chains to the hydration water in ConA amyloid fibrils has been proposed as the mechanism responsible for the observed enhancement of protein side-chain fluctuations [30].

The structural information obtained here on ConA fibrils by the combined use of FT-IR and FT-Raman in the MIR spectral region can be summarized as follows:

- As revealed by FT-IR spectra, the non β -sheet fraction of proteins in ConA fibrils maintains the native structural state upon fibrillation.
- Assignment of peaks at about 1690 cm^{-1} and 1620 cm^{-1} to fibril fingerprints is confirmed also for Raman spectra whose comparison with

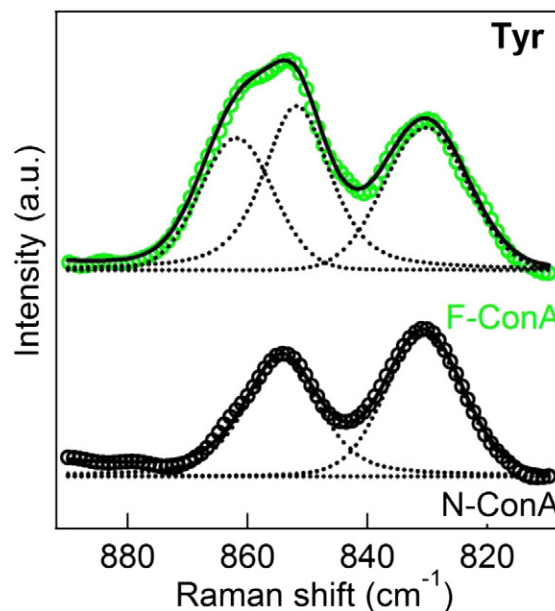


Fig. 4. Tyrosine Fermi doublet of native N-ConA and F-ConA. The tyrosine side chain generates a pair of distinctive Raman bands (a Fermi doublet near 860 and 830 cm^{-1}) whose relative intensities are diagnostic of hydrogen bonding states of the phenolic acceptor and donor atoms. The spectra show that while fibrillar aggregation occurs in ConA, the intensity ratio (R_{Tyr}) between the two peaks undergoes a significant change going from a value under 1 ($R_{\text{Tyr}}(\text{N-ConA}) = 0.75$) to values greater than 1 ($R_{\text{Tyr}}(\text{F-ConA}) = 1.1$). This hints at the possible exposure of tyrosines to the solvent.

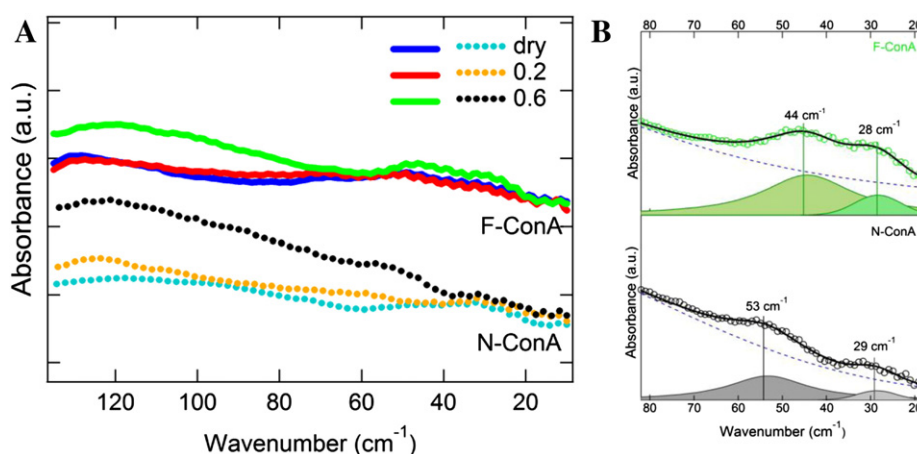


Fig. 5. (A) THz absorption spectra of native (N-) and fibrillar (F-) ConA powders at the hydration levels $h = 0$, $h = 0.2$ and $h = 0.6$. Since the absorbance values of F- and N-ConA were comparable, a constant baseline was added to F-ConA spectra and data were reported in arbitrary units to better show spectral shape differences. (B) Peak position evaluation in N- and F-ConA THz spectra at the maximum hydration level ($h = 0.6$).

FT-IR spectra reveals that Con A fibrillation occurs through the formation of β -sheets in antiparallel configuration.

- Aromatic chains (Tyr), hidden in hydrophobic regions in the native protein, partially expose to the surface of the fibrillar aggregate.

3.4. THz spectroscopy

In Fig. 5 we report the absorption spectra in the 20–130 cm^{-1} region at room temperature of dry ($h = 0$ $g_{\text{protein}}/g_{\text{H}_2\text{O}}$) ConA in native and fibrillar state in comparison with the same samples at hydration level $h = 0.2$ and $h = 0.6$. These experimental conditions allow characterizing hydration states where only water in the first hydration shell is present ($h = 0.2$) and where bulk water contribution is also detectable ($h = 0.6$). As can be seen critical difference exists between N-ConA and F-ConA sample, which are emphasized upon increasing hydration. The larger differences are observed in the region between 40 and 80 cm^{-1} . The spectra of dry powders appear almost flat with a small feature around 30 cm^{-1} , which is present in both protein states. As the hydration state of the samples is increased, an increase of the absorbance with frequencies is observed for both N- and F-ConA. This results in the growth of the overall slope of spectra. This effect is ascribable to the growth of water content in the sample since H-bonds in liquid water are known to absorb between 100 and 200 cm^{-1} [49]. At increasing hydration the appearance of two low energy absorptions in the region between 20 and 60 cm^{-1} occurs, being more evident in the case of F-ConA. Specifically, these narrow features are found around 53 and 29 cm^{-1} for N-ConA and around 44 and 28 cm^{-1} for F-ConA (Fig. 2B). The assignment in the literature of these features is not univocal. Few studies on protein systems in different states (powder, solution, crystals) have brought to different interpretations [18,25,49,50], assigning those peaks to both water and protein modes. The comparison between samples in fibril and native state and at different hydrations adds new gussets of knowledge to this issue. Indeed, the observation that the intensity of both features increases while hydration increases establishes their strict dependence on the hydration state and suggests that they could originate from hydration water absorption modes. This interpretation is in line with previous studies [50]. The same interpretation was given for the peak at lower frequency (around 29 cm^{-1}) [50]. This feature appears at the same spectral position for both N- and F-ConA, resulting to be structure independent in the present experimental conditions. A closer observation of spectra at $h = 0.6$ indicates that the feature found at about 53 cm^{-1} in N-ConA is red shifted to

44 cm^{-1} in the fibrillar state, thus suggesting a possible change in the protein–water interaction upon fibril formation that results in a softening of this vibrational mode.

This observation seems to reveal the enhancement of the softness of the hydration water spanning network occurring upon fibrillation.

4. Conclusions

In this work we presented a combined use of FT-MIR and FT-Raman spectroscopy to give structural highlights on amyloid fibrils. We provided the Raman experimental evidence for β -sheet mode splitting resulting from vibrational coupling between peptides, thus confirming calculated Raman peak assignments for amyloid aggregate samples. We observed that in ConA fibrils all the β -sheet active modes are clearly observed in a single Raman experiment. The coupling of IR and Raman analysis allowed us to obtain details on the reciprocal orientation of β -strands building up fibrils together with clear structural information on the solvent exposure of aromatic side chains upon fibril formation.

The results obtained in THz region, supported by the structural assignments made with MIR techniques, revealed specific features of amyloid fibrils in the low frequency spectral range. In particular, significant differences in the frequency of hydration water modes in the amyloid state of ConA with respect to the native state were found. Present results encourage further studies to obtain generalization of the attribution of the THz signals observed here.

We suggest that an extension of the present approach to micro-spectroscopies would enable a detailed structural characterization of amyloid plaques directly on tissues, recognize features of different aggregate deposits and furnish a rapid and detailed screening tool for amyloid-connected injuries.

Acknowledgment

Authors thank the members of the Molecular Biophysics and Soft Matter group <http://fisicaechemica.unipa.it/biophysicsmol/> Prof. Antonio Cupane and Prof. Maurizio Leone, University of Palermo, for useful discussion. We wish to thank Dr. Simonpietro Agnello for the consulting in Raman spectroscopy instrumentation. The financial supports of the University of Palermo (FFR-program 2012-ATE-0116) and of Elettra Sincrotrone of Trieste (proposal number 20125010) are also acknowledged.

References

- [1] B.H. Toyama, J.S. Weissman, Amyloid structure: conformational diversity and consequences, *Annu. Rev. Biochem.* 80 (2011) 557–585. <http://dx.doi.org/10.1146/annurev-biochem-090908-120656>.
- [2] J.C. Rochet, P.T. Lansbury Jr., Amyloid fibrillogenesis: themes and variations, *Curr. Opin. Struct. Biol.* 10 (2000) 60–68. [http://dx.doi.org/10.1016/S0959-440X\(99\)00049-4](http://dx.doi.org/10.1016/S0959-440X(99)00049-4).
- [3] C.M. Dobson, Protein folding and misfolding, *Nature* 426 (2003) 884–890. <http://dx.doi.org/10.1038/nature02261>.
- [4] J.L. Jimenez, E.J. Nettleton, M. Bouchard, C.V. Robinson, C.M. Dobson, H.R. Saibil, The protofibril structure of insulin amyloid fibrils, *Proc. Natl. Acad. Sci. U. S. A.* 99 (14) (2002) 9196–9201. <http://dx.doi.org/10.1073/pnas.142459399>.
- [5] A.J. Baldwin, T.P.J. Knowles, G.G. Tartaglia, A.W. Fitzpatrick, G.L. Devlin, S.L. Shammass, C.A. Waudby, M.F. Mossuto, S. Meehan, S.L. Gras, J. Christodoulou, S.J. Anthony-Cahill, P.D. Barker, M. Vendruscolo, C.M. Dobson, Metastability of native proteins and the phenomenon of amyloid formation, *J. Am. Chem. Soc.* 133 (2011) 14160–14166. <http://dx.doi.org/10.1021/ja2017703>.
- [6] T.P.J. Knowles, M.J. Buehler, Nanomechanics of functional and pathological amyloid materials, *Nat. Nanotechnol.* 6 (2011) 469–479. <http://dx.doi.org/10.1038/nnano.2011.102>.
- [7] S. Ketten, Z. Xu, B. Ihle, M.J. Buehler, Nanoconfinement controls stiffness, strength and mechanical toughness of β -sheet crystals in silk, *Nat. Mater.* 9 (2010) 359–367. <http://dx.doi.org/10.1038/nmat2704>.
- [8] G. Yoon, J. Kwak, J.L. Kim, S. Na, K. Eom, Mechanical characterization of amyloid fibrils using coarse-grained normal mode analysis, *Adv. Funct. Mater.* 21 (2011) 3454–3463. <http://dx.doi.org/10.1002/adfm.201002493>.
- [9] Z. Xu, R. Paparcone, M.J. Buehler, Alzheimer's A β (1–40) amyloid fibrils feature size-dependent mechanical properties, *Biophys. J.* 98 (10) (2010) 2053–2062. <http://dx.doi.org/10.1016/j.bpj.2009.12.4317>.
- [10] Y. Levy, E. Duboué-Dijon, F. Sterpone, J.T. Hynes, D. Laage, Biomolecular hydration dynamics: a jump model perspective, *Chem. Soc. Rev.* 42 (2013) 5672–5683. <http://dx.doi.org/10.1039/C3CS60091B>.
- [11] A.C. Fogarty, D. Laage, Water dynamics in protein hydration shells: the molecular origins of the dynamical perturbation, *J. Phys. Chem. B* 118 (28) (2014) 7715–7729. <http://dx.doi.org/10.1021/jp409805p>.
- [12] R. Tycko, Solid-state NMR studies of amyloid fibril structure, *Annu. Rev. Phys. Chem.* 62 (2011) 279–299. <http://dx.doi.org/10.1146/annurev-physchem-032210-103539>.
- [13] O.N. Antzutkin, R.D. Leapman, N.W. Rizzo, J. Reed, R. Tycko, Multiple quantum solid-state NMR indicates a parallel, not antiparallel, organization of β -sheets in Alzheimer's β -amyloid fibrils, *Proc. Natl. Acad. Sci. U. S. A.* 97 (24) (2000) 13045–13050.
- [14] R. Zhang, X. Hu, H. Khant, Interprotofibril interactions between Alzheimer's A β (1–42) peptides in amyloid fibrils revealed by cryoEM, *Proc. Natl. Acad. Sci. U. S. A.* 106 (12) (2009) 4653–4658. <http://dx.doi.org/10.1073/pnas.0901085106>.
- [15] J. Kong, S. Yu, Fourier Transform infrared spectroscopic analysis of protein secondary structures, *Acta Biochim. Biophys. Sin.* 39 (8) (2007) 549–559.
- [16] M. van de Weert, P.I. Haris, W.E. Hennink, D.J. Crommelin, Fourier transform infrared spectrometric analysis of protein conformation: effect of sampling method and stress factors, *Anal. Biochem.* 297 (2) (2001) 160–169.
- [17] F. Piccirilli, S. Mangialardo, P. Postorino, L. Baldassarre, S. Lupi, A. Perucchi, Sequential dissociation of insulin amyloids probed by high pressure Fourier transform infrared spectroscopy, *Soft Matter* 8 (2012) 11863–11870.
- [18] G. Acbas, K.A. Niessen, E.H. Snell, A.G. Markelz, Optical measurements of long-range protein vibrations, *Nat. Commun.* 5 (2014) 3076.
- [19] D.A. Turtto, H.M. Senn, T. Harwood, A.J. Lapthorn, E.M. Ellis, K. Wynne, Terahertz underdamped vibrational motion governs protein-ligand binding in solution, *Nat. Commun.* 5 (2014) 3999.
- [20] I. Lundholm, W.Y. Walgren, F. Piccirilli, P. Di Pietro, A. Duelli, O. Berntsson, S. Lupi, A. Perucchi, Terahertz absorption of illuminated photosynthetic reaction center solution: a signature of photoactivation? *RSC Adv.* 4 (49) (2014) 25502–25509.
- [21] J.R. Knab, J.Y. Chen, A.G. Markelz, Terahertz measurements of protein relaxation dynamics, *Proc. IEEE* 95 (2007) 1605–1610.
- [22] A.G. Markelz, Terahertz dielectric sensitivity of biomolecular structure and function, *IEEE J. Sel. Top. Quant. Electron.* 14 (2008) 180–190.
- [23] A.G. Markelz, S. Whitmire, J. Hillebrecht, R. Birge, THz time domain spectroscopy of biomolecular conformational modes, *Phys. Med. Biol.* 47 (21) (2002) 3797.
- [24] E. Castro-Camus, M.B. Johnston, Conformational changes of photoactive yellow protein monitored by terahertz spectroscopy, *Chem. Phys. Lett.* 4 (2008) 289–293.
- [25] R. Liu, M. He, R. Su, Y. Yu, W. Qi, Z. He, Insulin amyloid fibrillation studied by terahertz spectroscopy and other biophysical methods, *Biochem. Biophys. Res. Commun.* 391 (1) (2010) 862–867.
- [26] G. Schirò, V. Vetri, C.B. Andersen, F. Natali, M.M. Koza, M. Leone, A. Cupane, The boson peak of amyloid fibrils: probing the softness of protein aggregates by elastic neutron scattering, *J. Phys. Chem. B* 118 (11) (2014) 2913–2923.
- [27] V. Vetri, R. Carrota, P. Picone, M. Di Carlo, V. Militello, Concanavalin A aggregation and toxicity on cell cultures, *Biochim. Biophys. Acta* 1804 (2010) 173–183. <http://dx.doi.org/10.1016/j.bbapap.2009.09.013>.
- [28] J. Emsley, H.E. White, B.P. O'Hara, G. Oliva, N. Srinivasan, I.J. Tickle, T.L. Blundell, M.B. Pepys, S.P. Wood, Structure of pentameric human serum albumin P component, *Nature* 367 (1994) 338–345. <http://dx.doi.org/10.1038/367338a0>.
- [29] V. Vetri, G. Ossato, V. Militello, M.A. Dignam, M. Leone, E. Gratton, Fluctuation methods to study protein aggregation in live cells: concanavalin A oligomers formation, *Biophys. J.* 100 (2011) 774–783. <http://dx.doi.org/10.1016/j.bpj.2010.11.089>.
- [30] G. Schirò, V. Vetri, B. Frick, V. Militello, M. Leone, A. Cupane, Neutron scattering reveals enhanced protein dynamics in concanavalin A amyloid fibrils, *J. Phys. Chem. Lett.* 3 (2012) 992–996. <http://dx.doi.org/10.1021/jz300082x>.
- [31] V. Arluison, C. Mura, M. Romero Guzmán, J. Liquier, O. Pellegrini, M. Gingery, P. Régner, S. Marco, Three-dimensional structures of fibrillar Sm proteins: Hfq and other Sm-like proteins, *J. Mol. Biol.* 356 (2006) 86–96.
- [32] R.I. Litvinov, D.A. Faizullin, Y.F. Zuev, J.W. Weisel, The α -helix to β -sheet transition in stretched and compressed hydrated fibrin clots, *Biophys. J.* 103 (5) (2012) 1020–1027. <http://dx.doi.org/10.1016/j.bpj.2012.07.046>.
- [33] S. Lupi, A. Nucara, A. Perucchi, P. Calvani, M. Ortolani, L. Quaroni, M. Kiskinova, Performance of SSSI, the infrared beamline of the ELETTRA storage-ring, *J. Opt. Soc. Am. B* 24 (2007) 959. <http://dx.doi.org/10.1364/JOSAB.24.000959>.
- [34] Y. Jiang, C. Li, X. Nguyen, S. Muzammil, E. Towers, J. Gabrielson, L. Narhi, Qualification of FTIR spectroscopic method for protein secondary structural analysis, *J. Pharm. Sci.* 100 (11) (2011) 4631–4641. <http://dx.doi.org/10.1002/jps.22686>.
- [35] F. Piccirilli, S. Mangialardo, P. Postorino, S. Lupi, A. Perucchi, FT-IR analysis of the high pressure response of native insulin assemblies, *J. Mol. Struct.* 1050 (2013) 159–165. <http://dx.doi.org/10.1016/j.molstruc.2013.07.028>.
- [36] A. Barth, C. Zscherp, What vibrations tell about proteins, *Q. Rev. Biophys.* 35 (4) (2002) 369–430. <http://dx.doi.org/10.1017/S0033583502003815>.
- [37] Y.N. Chirgadze, N.A. Nevskaya, Infrared spectra and resonance interactions in amide I vibration of the parallel chain pleated sheet, *Biopolymers* 15 (1976) 627–636. <http://dx.doi.org/10.1002/bip.1976.360150402>.
- [38] E. Cerf, R. Sarroukh, S. Tamamizu-Kato, L. Breydo, S. Derclaye, Y.F. Dufrène, V. Narayanaswami, E. Goormaghtigh, J.M. Ruysschaert, V. Raussens, Antiparallel β -sheet: a signature structure of the oligomeric amyloid β -peptide, *Biochem. J.* 421 (3) (2009) 415–423. <http://dx.doi.org/10.1042/BJ20090379>.
- [39] H. Fabian, W. Mantele, Infrared spectroscopy of proteins, *Handbook of Vibrational Spectroscopy*, Wiley & Sons Ltd, 2006. <http://dx.doi.org/10.1002/0470027320.s8201>.
- [40] M. Marin-Argany, A.M. Candel, J. Murciano-Calles, J.C. Martinez, S. Villegas, The interconversion between a flexible β -sheet and a fibril β -arrangement constitutes the main conformational event during misfolding of PSD95-PDZ3 domain, *Biophys. J.* 103 (4) (2012) 738–747.
- [41] K.D. Hardman, C.F. Ainsworth, Structure of concanavalin A at 2.4-Å resolution, *Biochemistry* 11 (1972) 4910–4919.
- [42] Yu.N. Chirgadze, N.A. Nevskaya, Infrared spectra and resonance interaction of amide-I vibration of the antiparallel-chain pleated sheet, *Biochemistry* 15 (4) (1976) 607–625.
- [43] J. Kubelka, T.A. Keiderling, Differentiation of β -sheet-forming structures: ab initio-based simulations of IR absorption and vibrational CD for model peptide and protein β -sheets, *J. Am. Chem. Soc.* 123 (48) (2001) 12048–12058. <http://dx.doi.org/10.1021/ja0116627>.
- [44] P. Bour, T.A. Keiderling, Structure, spectra and the effects of twisting of β -sheet peptides. A density functional theory study, *J. Mol. Struct.* 675 (2004) 95–105. <http://dx.doi.org/10.1016/j.theochem.2003.12.046>.
- [45] V. Vetri, C. Canale, A. Relini, L. Librizzi, V. Militello, A. Gliozzi, M. Leone, Amyloid fibrils formation and amorphous aggregation in concanavalin A, *Biophys. Chem.* 125 (2007) 184–190.
- [46] S. Mangialardo, F. Piccirilli, A. Perucchi, P. Dore, P. Postorino, Raman analysis of insulin denaturation induced by high-pressure and thermal treatments, *J. Raman Spectrosc.* 43 (2012) 692–700. <http://dx.doi.org/10.1002/jrs.3097>.
- [47] N.T. Yu, C.S. Liu, D.C. O'Shea, Laser Raman spectroscopy and the conformation of insulin and proinsulin, *J. Mol. Biol.* 70 (1972) 117. [http://dx.doi.org/10.1016/0022-2836\(72\)90167-2](http://dx.doi.org/10.1016/0022-2836(72)90167-2).
- [48] Z. Arp, D. Autrey, J. Laane, S.A. Overman, G.J.J. Thomas, Tyrosine Raman signatures of the filamentous virus Ff are diagnostic of non-hydrogen-bonded phenoxyls: demonstration by raman and infrared spectroscopy of p-cresol vapor, *Biochemistry* 40 (2001) 2522–2529.
- [49] M. Heyden, J. Sun, S. Funkner, G. Mathias, H. Forbert, M. Havenith, D. Marx, Dissecting the THz spectrum of liquid water from first principles via correlations in time and space, *PNAS* 107 (27) (2010) 12068–12073.
- [50] K.D. Moeller, G.P. Williams, S. Steinhäuser, C. Hirschmugl, J.C. Smith, Hydration-dependent far-infrared absorption in lysozyme detected using synchrotron radiation, *Biophys. J.* 61 (1992) 277. [http://dx.doi.org/10.1016/S0006-3495\(92\)81834-9](http://dx.doi.org/10.1016/S0006-3495(92)81834-9).